Spermine-Induced Aggregation of DNA, Nucleosome, and Chromatin

E. Raspaud,* I. Chaperon,# A. Leforestier,* and F. Livolant*
*Laboratoire de Physique des Solides, CNRS UMR 8502, Université Paris Sud, 91405 Orsay Cedex, France, and # Service de Biochimie et Génétique Moléculaire, CEA/Saclay, 91191 Gif-sur-Yvette, France

ABSTRACT We have analyzed the conditions of aggregation or precipitation of DNA in four different states: double-stranded DNA (dsDNA), single-stranded DNA (ssDNA), mononucleosome core particles (NCP), and H1-depleted chromatin fragments (ChF) in the presence of the multivalent cation spermine (4+). In an intermediate regime of DNA concentration, these conditions are identical for the four states. This result demonstrates that the mechanism involved is general from flexible chains to rigid rods and quasi-colloidal states. It is dominated by local electrostatic attractions that are considered, for instance, by the "ion-bridging" model. The onset of precipitation does not require the electroneutrality of the DNA chains. Above a given spermine concentration dsDNA aggregates remain neutral, whereas NCP aggregates turn positively charged. The difference is thought to originate from the extension of the positively charged proteic tails of the NCP. This suggests that local fluctuations of polyamine concentrations can induce either positively or negatively charged chromatin domains.

INTRODUCTION

Long DNA is naturally compacted in a dense form in most biological systems. The DNA compact form (globular form) may result from a confinement (inside a viral capsid or a nuclear envelope) and/or from the presence of a compacting agent (polyamines or basic proteins). In vitro, the role of polyamines and other multivalent cations in this compacting process has been extensively studied (see Bloomfield et al. (1994) and further references therein). These cations act as electrostatic bridges between the DNA phosphate charges, thus inducing the formation of globules (single collapsed chains), aggregates, and/or macroscopic rich DNA phases. This process is not restricted to double-stranded DNA chains, but appears to be general for all highly charged linear chains, from rodlike biopolymers (actin filaments, microtubules, etc.) (Tang et al., 1996) to flexible synthetic polyelectrolytes such as poly(styrene sulfonate) (Delsanti et al., 1994). In the latter case, experimental conditions required to precipitate polymers have been explained by the "ion-bridging" model developed by Olvera de la Cruz et al. (1995). Based on this model, analytical expressions of the instability conditions of a DNA solution have been proposed (Raspaud et al., 1998). This approach takes only into account the monovalent counterions of DNA and the added multivalent ions. In the case where all the multivalent ions are condensed along the chains, with no condensed monovalent ions, the spinodal equation reads

$$C_+ = (C_u/z)(1 - A \times C_u^{1/4} + B \times C_u^{1/2}) \qquad (1)$$

where C_+ is the concentration of multivalent ions and C_u is the concentration of monovalent charged units of the polyelectrolytes. These two concentrations are expressed in particles/Å^3 units (1 mM corresponds to 6×10^{-7} particles/Å^3). The constants A and B are numerical constants that depend solely on the multivalent ions valence z and on the Bjerrum length l_B: $A = (z - 1) \times (2\ \pi\ l_B^3)^{1/4} \times [(1 - 1/z)/z]^{1/2}$ and $B = (z - 1)^2 \times (\pi\ l_B^3)^{1/2} \times (1 - 2/z)/(2^{1/2}\ z)$. For instance, in water $l_B = 7$ Å and for spermine cations $z = 4$, $A = 8.85$, and $B = 26.1$. This model relies on a few assumptions and predictions:

1. The degree of polymerization or the molecular weight of the chains can be neglected because the term of translation entropy loss, characteristic of polymeric solutions, is predicted negligible compared to the electrostatic interactions terms;
2. The charge density of the chains or of the charged objects is irrelevant. The basic hypothesis of this model concerns solutions of highly charged polyelectrolytes, in the large meaning of the word, where one expects ion condensation in the vicinity of the polyelectrolyte;
3. This equation is applicable regardless of the charged object geometry. Since the electrostatic attractions are predicted to be local and predominant, the polymeric state of the charged object vanishes;
4. The polyelectrolytes are expected to still be charged when the system becomes unstable, since the instability is assumed to occur below the electroneutrality ($C_+ = C_u/z$).

In a previous work, we have shown the applicability of this model to solutions of double-stranded DNA (dsDNA) precipitated by spermine, and verified point 1, i.e., the independence of the molecular weight (Raspaud et al., 1998). In the present work, we investigate the four points as a whole. Our first aim is to compare the precipitation conditions of linear molecules with different charge densities, such as dsDNA and single-stranded DNA (ssDNA) molecules (point 2). For ssDNA chains, the relevant structural parameter ξ (defined in the Background section) is of

Received for publication 2 February 1999 and in final form 19 May 1999.
Address reprint requests to Dr. Eric Raspaud, Laboratoire de Physique des Solides, CNRS UMR 8502, Université Paris Sud, 91405 Orsay Cedex, France. Tel.: 33-1-69-15-6087; Fax: 33-1-69-15-6086; E-mail: raspaud@lps.u-psud.fr.

0006-3495/99/09/1547/09 $2.00

the order of 1.8 depending on the pH values (Record et al., 1976). In comparison, ξ equals 4.2 for dsDNA. The second aim (point 3) is to extend this comparison to the case of nucleosome core particles (NCP) and H1-depleted chromatin in order to generalize the understanding of this process. Let us recall that NCP are formed by coiling a portion of 146-bp DNA around a central proteic octamer composed of two copies of each histone (H2A, H2B, H3, and H4). The overall particle, of molecular mass 2.08×10^5 g/mol, can be described as a wedge-shaped cylinder, 105 Å in diameter (d) and 57 Å in height (h) (Luger et al., 1997). As their anisotropic factor h/d equals 1.84, they cannot be considered as elongated cylinders, as in the case of linear polyelectrolytes ($h/d \gg 1$), but should rather be assimilated—in a first approximation—to spheres ($h/d = 1$) with charges localized at the surface. In H1-depleted chromatin, NCP are linked together by a linker DNA, whose length may vary from ~20 to 100 bp to form the nucleosomic fiber. In our experiments, we use calf thymus chromatin whose linker length is in the range of 45 bp (van Holde, 1989). Finally, the last point (4) will be tested by electrophoretic experiments on dsDNA and NCP aggregates.

MATERIALS AND METHODS

Double-stranded DNA

Fragments (146 bp) were obtained as described in Sikorav et al. (1994) from a selective digestion of calf thymus chromatin (Strzelecka and Rill, 1987). The molecular population is, however, polydisperse: the length of the fragments ranges from 50 to 10^3 basepairs. The DNA solutions were extensively dialyzed against a solution of TE buffer (10 mM Tris HCl, 1 mM EDTA, pH 7.6). NaCl and spermine (4 HCl; Fluka) were dissolved in the same buffer. We recall that 3 mM DNA phosphate corresponds to 1 mg/ml DNA.

Single-stranded DNA

Studies were performed with 72 and 118 base-long oligonucleotides obtained from Eurogentec (respectively, nucleotides 4878–4949 and 4760–4877 of the plus strand of ϕX174). The oligonucleotides were 5′ end-labeled with T4 polynucleotide kinase using γ^{32}P-ATP, purified by gel filtration on a Sephadex G-50 column (Pharmacia) and diluted in 2 mM NaCl (pH 5.8).

Nucleosome core particles and chromatin fragments preparation

Mononucleosome core particles (NCP) were obtained by selective digestion of H1-depleted chromatin with micrococcal nuclease (Pharmacia), followed by purification by gel chromatography over a Sephacryl S 300 HR column (Pharmacia), as described in Leforestier and Livolant (1997). The purity of the collected fraction and the core particle integrity were checked by retardation gel electrophoresis on a 7.5% polyacrylamide gel. NCP were dialyzed against TE buffer (10 mM Tris-HCl, 1 mM EDTA, pH 7.1) in presence of 5 or 75 mM NaCl, and concentrated by ultrafiltration under nitrogen pressure throughout a porous membrane (Amicon YM 100). This stock solution ($C_{NCP} > 100$ mg/ml) was stored at 4°C.

To prepare chromatin fragments (ChF), native calf thymus chromatin was partially digested with micrococcal nuclease (Pharmacia). Histone H1 were then removed with CM-Sephadex (Pharmacia). The H1-depleted chromatin fragments were extensively dialyzed against TE pH 7.1 with 5 mM NaCl, concentrated to 36 mg/ml by ultrafiltration in microconcentrator tubes (Amicon, centricon 100), and stored at 4°C. The histone composition of chromatin was checked by SDS gel electrophoresis on 15% acrylamide gels, and the length of chromatin fragments estimated by agarose gel electrophoresis. The population of chromatin fragments is heterogeneous: it is centered around 6- to 8-mers and varies from 1 to ~17 nucleosome repeats.

Phase diagram determination

The concentration C_{precip} corresponds to the spermine concentration for which the molecules start to precipitate (Raspaud et al., 1998). These values are given within an interval (whose limits correspond to the point where no precipitation has occurred and that where aggregation has been detected). At low concentrations (<0.5 mg/ml), samples of dsDNA, NCP, and ChF were slowly vortexed after spermine addition, incubated at room temperature for 15 min minimum, and centrifuged at $11{,}000 \times g$ for 7 min, which accelerates the precipitation process. The concentration in the supernatant was determined by measurements of the absorbance at 260 nm. For the higher concentrations (≥0.5 mg/ml), C_{precip} was determined by visual inspection after successive addition of spermine, and vortexing. The reversibility of the aggregation allows us to use this simple method.

For ssDNA solutions, after mixing with spermine, the samples were incubated during 30 min and centrifuged at $17{,}000 \times g$ for 5 min. The amount of aggregated ssDNA was determined by measurements of the radioactivity of the supernatant, as described in Chaperon and Sikorav (1998).

Electrophoretic measurements

The mobility of dsDNA and NCP aggregates was determined by electrophoretic measurements performed with a Delsa 440 SX instrument (Coulter). This technique measures the electrophoretic mobility U of particles submitted to an electric field E directly in solution. For particles of effective charge Q, the mobility is given by the relation $U = Q/f$, with f the frictional coefficient of the particle with the liquid medium. One has to keep in mind that during the particles movement, a layer of the surrounding liquid is drained so that the measured electrophoretic mobility corresponds to the mobility of the particles with their fixed liquid layers. In other words, the effective charge Q corresponds to the particle charge reduced by the charge of the condensed ions present in this layer.

In electrophoretic light scattering measurements, the photon-counting heterodyne correlation function is measured and Fourier-transformed. The Fourier transform gives the power spectrum $S(\omega)$, which has a Lorentzian form centered at $\omega_0 + \Delta\omega$, with ω_0 the frequency of the incident beam. The electrophoretic mobility U is detected through the frequency shift $\Delta\omega$, similar to the Doppler effect shift. This shift is the difference between the frequency of the light scattered at an angle θ (or at a transfer vector $q = (4\pi n/\lambda) \sin \theta/2$, with n the refractive index of the medium) and that of the incident beam. It can be written as $\Delta\omega = q\, U\, E \cos(\Theta)$, with Θ the angle between the electric field and the transfer vector. The shift frequency $\Delta\omega$ has been experimentally measured at four angles for each sample after a calibration with a suspension of modified polystyrene latex spheres ($U = -4.1 \times 10^{-8}$ m^2/V.s.). In our case and at the studied polyelectrolyte concentrations, it was not possible to determine the electrophoretic mobility of the samples outside of the precipitation range. This may be explained by a scattered intensity too weak to be measured at these concentrations by the apparatus.

Fig. 1 *a* shows the power spectra $S(\omega)$ measured for an NCP solution [$C_{\text{access. phosphate}}$ (hereafter referred to as C_{ap}) = 41 μM and $C_{spermine}$ (hereafter referred to as C_{sper}) = 10 mM] at the four angles (8.9°, 17.6°, 26.3°, and 35.2°). Taking into account the θ dependence of $\Delta\omega$, one obtains the distribution function of the electrophoretic mobility of the NCP aggregates (Fig. 1 *b*). For each angle, this function may be fitted by a Lorentzian function centered on a mobility value that is found independent of the angle. In the present case, the measured mobility U is positive, indicating a positive charge of the aggregates.

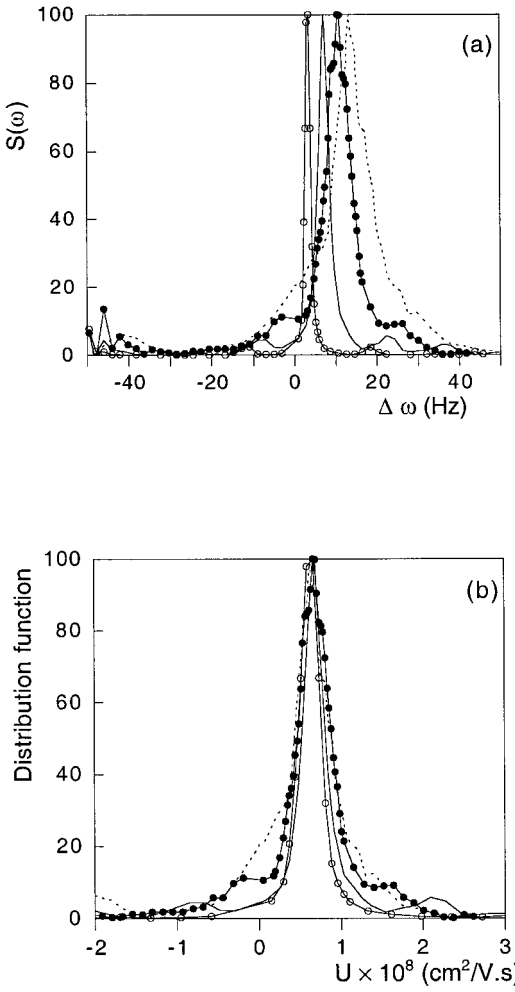

FIGURE 1 Electrophoretic light scattering spectra measured at different scattering angles $\theta = 8.9°$ (○), 17.6° (*solid line*), 26.3° (●), and 35.2° (*dashed line*). The sample is a solution of NCP/spermine diluted at concentrations $C_{ap} = 41\ \mu M$ and $C_{sper} = 10$ mM. The spectra are plotted as a function of the shift frequency $\Delta\omega = \omega - \omega_0$, with ω_0 the frequency of the incident beam (*a*). (*b*) Electrophoretic mobility deduced from $\Delta\omega$, θ, and the applied electric field strength. The spectra may be fitted by a Lorentzian centered on a value independent of the angle. This value U corresponds to the average electrophoretic mobility of the aggregates. In the present case, U is positive, which indicates a positive charge of the aggregates.

EXPERIMENTAL AND THEORETICAL BACKGROUND

In negatively charged polyelectrolytes, cations condense in the vicinity of the polyelectrolyte in order to reduce the electrostatic repulsion effects. Due to the large translation entropy loss of these condensed ions, the fraction of condensed ions will be limited. This situation can be theoretically considered in the case of linear and spherical polyelectrolytes.

Counterion condensation in the case of linear polyelectrolytes

This situation has been analyzed, in particular by Manning, for polyelectrolytes considered as straight infinite lines in infinitely dilute solution (1978). The relevant structural parameter is the linear charge density ξ defined as $\xi = l_B/b$, where l_B corresponds to the Bjerrum length and b to the average spacing of the polyelectrolyte charges. The limiting fraction of condensed charges is predicted equal to $1 - 1/(z\xi)$, with z the counterion valence. Thus, according to Manning, for dsDNA ($b = 1.7$ Å; $\xi = 4.2$), the fraction of neutralized charges is equal to 76% in the presence of monovalent ions and to 94% in the presence of tetravalent cations only.

In the "ion-bridging" model proposed by Olvera de la Cruz et al. (1995) and used in Raspaud et al. (1998), the condensation of spermine in the vicinity of the chains is thought to locally reverse the phosphate charge and to create a local attractive electrostatic interaction between a phosphate charge that does not carry any condensed ion and one that does carry a spermine counterion. DNA precipitation results from the competition between initial monovalent counterions and added spermine to condense onto the polyelectrolytes. In the case where no extra monovalent salt is added, three regions were determined theoretically (Fig. 2) assuming the most simplified Manning's model. They are separated by the two limits (*dashed lines*) of equations $C_{sper}/C_{DNA\ phosphate}$ (hereafter referred to as C_{DNAp}) $= (1 - 1/z\xi)/z = 0.235$ and $C_{sper}/C_{DNAp} = (1 - 1/\xi)/z = 0.19$ with z the spermine valence (=4). The experimental values of the spermine concentration C_{precip} required for the precipitation of dsDNA have been reported on the same figure. Note that these experimental values have been obtained in the presence of a small amount of added monovalent salt (10 mM TE in the present case) to prevent denaturation of the molecule. The C_{precip} values are distributed in the three regions defined below:

In region c, $C_{sper}/C_{DNAp} > (1 - 1/z\xi)/z$, spermine cations are expected to be partly free and partly condensed along the DNA molecules. The fraction of condensed spermine cations being given by Manning's limit, the instability conditions are expected to be dependent on ξ. As the free spermine ions participate in the electrostatic screening, other energetic terms cannot be neglected. Indeed, the instability conditions were found to depend also on the molecular weight and on enthalpic terms, such as the classical excluded volume. In the limit of infinitely long chains and for an excluded volume equal to zero, the spermine concentrations at precipitation were theoretically found equal to $\alpha \times C_{DNAp} + \beta$, with $\alpha = 0.14$ and $\beta = 3.7 \times 10^{-4}$. This equation is in principle limited by the "no added monovalent salt" condition, but is still valid for concentrations of added monovalent salt smaller than the spermine concentration. Higher monovalent salt concentration leads to condensation of a fraction of these new cations. This decreases the number of condensed multivalent counterions, as described by the two-variable theory of Manning (1978). Despite the presence of added monovalent salt in our experiments, we will continue to

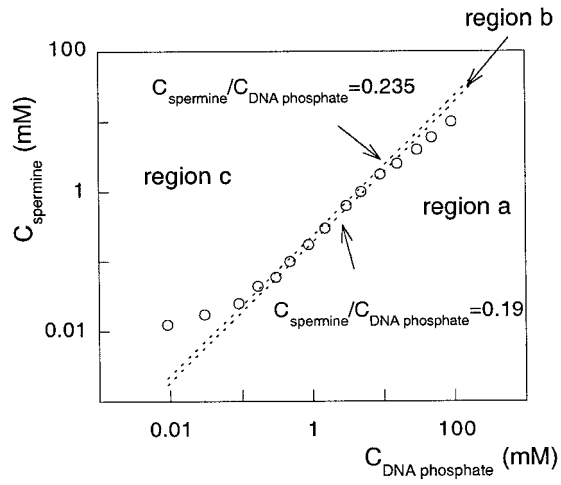

FIGURE 2 Concentration of spermine required to precipitate double-stranded DNA fragments of 150 basepairs diluted in a TE buffer pH 7.6, versus the DNA phosphate concentration. The two parallel dotted lines correspond to the equations $C_{sper}/C_{DNAp} = (1 - 1/z\xi)/z = 0.235$, and $C_{sper}/C_{DNAp} = (1 - 1/\xi)/z = 0.19$, and delimit the three theoretical regions a, b, and c (reproduced from Raspaud et al. (1998))

call this region "region c." Experimentally, at low DNA concentration, the multivalent ion concentration required to induce the collapse and/or the aggregation of dsDNA chains is found dependent on the molecular weight for short DNA chains, on the chemical species of the multivalent ions, and on the monovalent added salt concentration (cf. for instance Wilson and Bloomfield, 1979; Marquet et al., 1987; Pelta et al., 1996).

In the narrow region b, $(1 - 1/z\xi)/z > C_{sper}/C_{DNAp} > (1 - 1/\xi)/z$. All spermine cations are condensed along DNA chains and all initial monovalent counterions are free. This region corresponds to the case mentioned in the Introduction, where the instability conditions are only governed by the electrostatic interactions leading to expression 1. This theoretical prediction was found to be in very good agreement with the experimental data. Theoretically, the fraction of neutralized phosphates increases proportionally with the ratio C_{sper}/C_{DNAp} from 76 to 94%. Experimentally, this variation is not detectable, and the precipitation of dsDNA in this regime occurs on average for a constant ratio $C_{precip}/C_{DNAp} = 0.20 \pm 0.02$, leading to $80 \pm 8\%$ of neutralized phosphates. These conditions are independent of the dsDNA molecular weight, as expected theoretically, and also independent of the concentration of the added monovalent salt into the solution. Thus the added monovalent salt has no effect in this region b, which validates the relevance of the initial "no added monovalent salt" condition.

For linear polyelectrolytes with lower charge density, like ssDNA chains ($b = 4$ Å; $\xi = 1.8$), the two limits enclosing the region b are shifted to lower fractions C_{sper}/C_{DNA}: $(1 - 1/z\xi)/z = 0.215$, $(1 - 1/\xi)/z = 0.111$. It means that this region b should become more extended.

In region a, $C_{sper}/C_{DNA} < (1 - 1/\xi)/z$. One expects the precipitation to occur when both initial monovalent cations and added multivalent spermine are condensed on the molecule. This region is not considered here.

Counterion condensation in the case of spherical polyelectrolytes

As in the case of linear polyelectrolytes, the condensation of counterions around a spherical object results from a balance between the thermal energy and the reduction of the electrostatic interactions. Ion condensation in this geometry has been examined by Alexander et al. (1984) and Belloni (1982, 1985). In the case of monovalent ions and for spheres of radius a and structural charge Z_s, ion condensation occurs if $Z_s \geq 4\ Y/l_B$, where Y corresponds to the distance between the center of the sphere and a cutoff limit, below which the counterions are supposed to be condensed (Belloni, 1985). Following the Manning's notation, one has $Y = a + \Delta x$, with Δx the thickness of the spherical shell in which the cations are said to be "condensed." For highly charged spheres and in the absence of added salt, one expects an effective charge of the sphere $Z_{eff} = 4\ Y/l_B$. This is found in very good agreement with experiments on micellar solutions (Bucci et al., 1991).

In the case of NCP, the association of DNA with the histone core proteins neutralizes ~130–134 phosphate charges, leaving 158–162 charges accessible to polyamine counterions (structural charge $Z_s \cong 160$) (Khrapunov et al., 1997). Therefore, the relevant concentration becomes the concentration of accessible phosphates $C_{ap} = (160/292) \times C_{DNAp} \cong 0.55 \times C_{DNAp}$. This prefactor is in good agreement with the value calculated by Clark and Kimura (1990) using the data of magnesium binding to NCP (Watanabe and Iso, 1984). In principle, the determination of Δx requires sophisticated numerical calculations. Here, we have only evaluated a minimum effective charge of NCP. Assuming a radius of the NCP equivalent sphere $a \cong 50$ Å and a distance $Y \cong a$, the minimum of Z_{eff} is of the order of $Z_{eff} \cong 4\ a/l_B = 29$, giving at most 82% of DNA phosphates neutralized by counterion condensation. For multivalent counterions, this minimum effective charge is reduced by a factor $1/z$ (Belloni, 1982) leading to at most 96% of phosphates neutralized by spermine.

For spherical particles, the effective charge varies only with their size, which is finite. For linear polyelectrolytes, this effect is usually not taken into account (infinite line) except for short fragments (Ramanathan, 1988). For a long charged line of total structural charge Z_s, the total effective charge is simply given by the ratio $Z_{eff}/Z_s = 1/z\ \xi$, whereas for a charged sphere, this ratio may be approximated by $Z_{eff}/Z_s \sim a/(z\ l_B\ Z_s)$. Assuming a surface charge density $1/b^2$, this ratio varies as the product $Z_{eff}/Z_s \sim (1/z\ \xi) \times (b/a)$ and reduces to the above linear case when $b = a$.

Following these simple estimations of the NCP effective charge in the presence of mono and multivalent ions, one expects significant counterion condensation. In a first approximation, we shall assume that the fraction of phosphates neutralized by ion condensation in the case of dsDNA and NCP are of the same order of magnitude. This leads us to propose that the phase diagram (C_{sper} as a function of C_{DNA}) of NCP solutions can also be divided into three regions a, b, and c separated by two limits that can be considered identical to those of dsDNA in a first approximation.

RESULTS

Phase diagram

Precipitation conditions are summarized in Fig. 3 (ssDNA and dsDNA) and Fig. 4 (dsDNA, NCP, and ChF). The precipitation has been studied over more than four decades in DNA concentration in order to examine the different variations of C_{precip} as a function of C_{ap}. As mentioned in the Introduction, we have considered the accessible DNA phosphate fraction C_{ap} as the significant variable ($C_{ap} = C_{DNAp}$ for ss or dsDNA, $C_{ap} = 0.55 \times C_{DNAp}$ for NCP and $C_{ap} = 0.65 \times C_{DNAp}$ for ChF). In all cases, the data reveal the presence of at least two regimes of variation, located in the two theoretical regions b and c.

In the theoretical region c (at low C_{ap} values), the spermine concentrations required to induce the precipitation, C_{precip}, are found dependent on the molecular species, their molecular weight, and the concentration of added monovalent ions. Nevertheless, each series of data may be fitted by a linear relationship $C_{precip} = \alpha \times C_{ap} + \beta$, which tends to a constant value β for sufficiently diluted solutions. It is difficult to compare the values measured on the different molecular species, but it seems that more spermine must be added to the ssDNA and NCP solutions than to the dsDNA ones to induce the precipitation. This is in good agreement with the recent results reported by Saminathan et al. (1999). This difference could be explained by the difference of

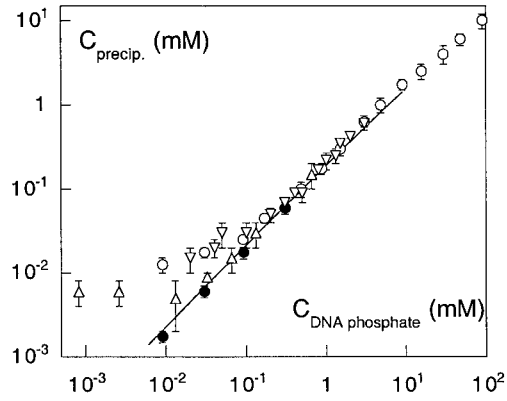

FIGURE 3 Comparison of the precipitation conditions for double-stranded DNA, diluted in: (○) TE buffer pH 7.6 and (●) 2 mM NaCl pH 5.1, and for single-stranded DNA, 72 (▽) and 118 (△) base-long, diluted in 2 mM NaCl pH 5.8. The full line corresponds to the theoretical prediction given by Eq. 1.

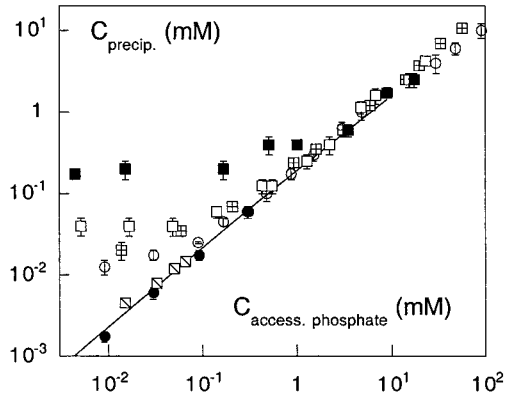

FIGURE 4 Precipitation conditions of double-stranded DNA diluted in a TE buffer pH 7.6 (○), in 2 mM NaCl pH 5.1 (●), of nucleosome core particles diluted in a TE buffer pH 7.1 + NaCl 5 mM (□), in a TE buffer pH 7.1 + NaCl 75 mM (■), and of chromatin fragments diluted in a TE buffer pH 7.1 + NaCl 5 mM (⊞). The symbols (⧅) correspond to calf thymus chromatin solutions and are deduced from Fig. 3 in Smirnov et al. (1988). The solid line corresponds to the theoretical prediction given by Eq. 1.

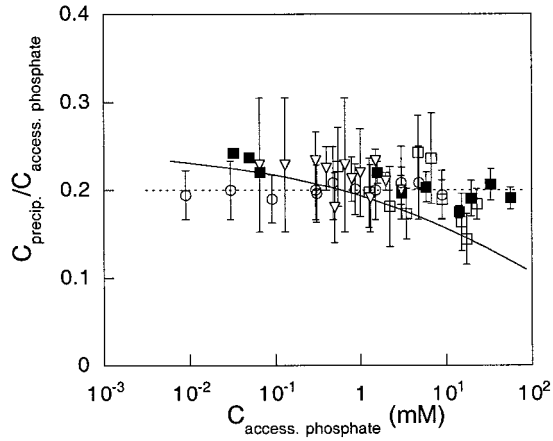

FIGURE 5 Ratio of the spermine concentration required to start the aggregation or the precipitation process to the DNA phosphate charges accessible to the spermine molecules. Within experimental precision, this ratio is found constant: $C_{precip}/C_{ap} = 0.20 \pm 0.02$, whatever the DNA concentration and the charged object. (○) Double-stranded DNA, (▽) single-stranded DNA, (□) nucleosome core particles, and (■) chromatin fragments. The solid line corresponds to the theoretical prediction (Eq. 1) and the dashed one to the constant value 0.2.

charge density and/or by a difference of nonelectrostatic and specific interactions between molecules and ions. The range of concentration (C_{ap}) described by this relationship extends when the monovalent ion concentration is increased, thus progressively reducing the second domain described below.

Our major result concerns the theoretical region b. In this region, all the data are superimposed on the theoretical line given by Eq. 1 (Figs. 3 and 4). As already explained, this domain of superimposition extends over a concentration range that depends on numerous parameters, namely the monovalent ion concentration (the lower the monovalent ion concentration, the more extended this domain) and the considered material (nature and molecular mass). The experimental points located in this region can be fitted by a constant ratio $C_{precip}/C_{ap} = 0.20 \pm 0.02$. This ratio is independent of the molecular weight, as illustrated by the comparison of ssDNA (72 and 118 bases ssDNA solutions in Fig. 3), chromatin fragments (short ones in our experiments, long ones in data reported by Smirnov et al., 1988; see Fig. 4), and dsDNA (Raspaud et al., 1998). This ratio is also independent of the added monovalent salt concentration (cf. the data of dsDNA and NCP on Fig. 4), which demonstrates that a condensation competition occurs between the multivalent ions and the monovalent counterions that initially maintain the electroneutrality of the polyelectrolytes. Moreover, these data confirm that the charge density and the geometry of the charged object do not influence the precipitation process. This will be discussed in detail below. For a more detailed analysis of this region, all relevant experimental points have been gathered on Fig. 5, where the ratio C_{precip}/C_{ap} is expressed as a function of C_{ap}. These values seem better described by a constant 0.2 value than by the theoretical curve (Eq. 1).

It must be noted that above a given spermine concentration, precipitation is suppressed independently of its concentration (data not shown). This spermine concentration, also called resolubilization concentration, was previously found independent of the dsDNA concentration (105 ± 10 mM) (Raspaud et al., 1998). In the present work, we find a spermine concentration of resolubilization of the order of 150 mM for 118 bases ssDNA and equal to 50 ± 10 mM for NCP (not measured for ChF).

Electrophoretic measurements

The mobilities U were measured over the spermine concentration range where aggregation occurs (Figs. 6 and 7). No significant changes of the mobility values have been observed during the 20 min after mixing. The variation of the electrophoretic mobilities U with the spermine concentration is different in the case of dsDNA and NCP. For dsDNA (Fig. 6 *a*), close to the "precipitation line," i.e., for low C_{sper} values, the mobility is negative, implying that the aggregates are negatively charged. The mobility, which is found independent of the dsDNA concentration, increases progressively with the spermine concentration. Above 2 mM spermine, no frequency shift of the power spectra $S(\omega)$ (cf. Methods section) can be detected by the apparatus and the mobility remains equal to zero.

For NCP solutions (Fig. 7 *a*), the variation of the electrophoretic mobility U is also the same for the two studied NCP concentrations (0.082 and 0.041 mM accessible phosphate). The negative mobility increases progressively with the spermine concentration and becomes zero around 1 mM spermine. Contrary to the dsDNA case, the mobility continues to increase with the addition of spermine and becomes positive, indicating that the charge of the aggregates

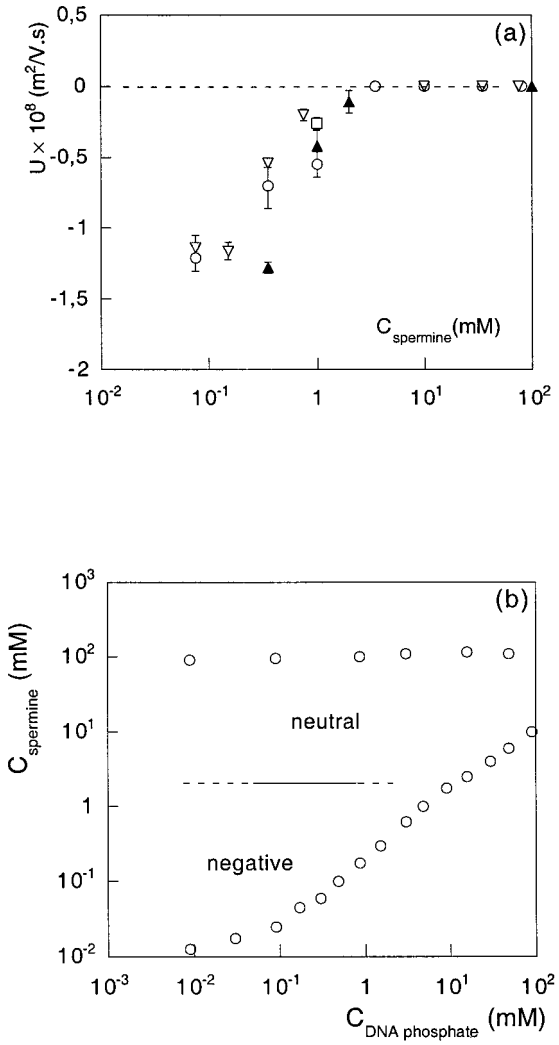

FIGURE 6 (*a*) Variation of the electrophoretic mobility of the aggregates of dsDNA with the spermine concentration in TE buffer. The concentrations of phosphate DNA in mM units are equal to: (▽) 0.075, (▲) 0.15, (○) 0.3, and (□) 0.75. The dotted line indicates the zero electrophoretic mobility value. Aggregates are negatively charged below 2 mM spermine and neutral above. (*b*) Surface charge of the dsDNA aggregates determined by electrophoretic measurements and reported in the phase diagram. The electrophoretic mobility becomes nil at 2 mM spermine for $0.075 > C_{DNAp}$ (mM) > 0.75 (*solid line*). We have extrapolated this line on both sides (*dashed line*).

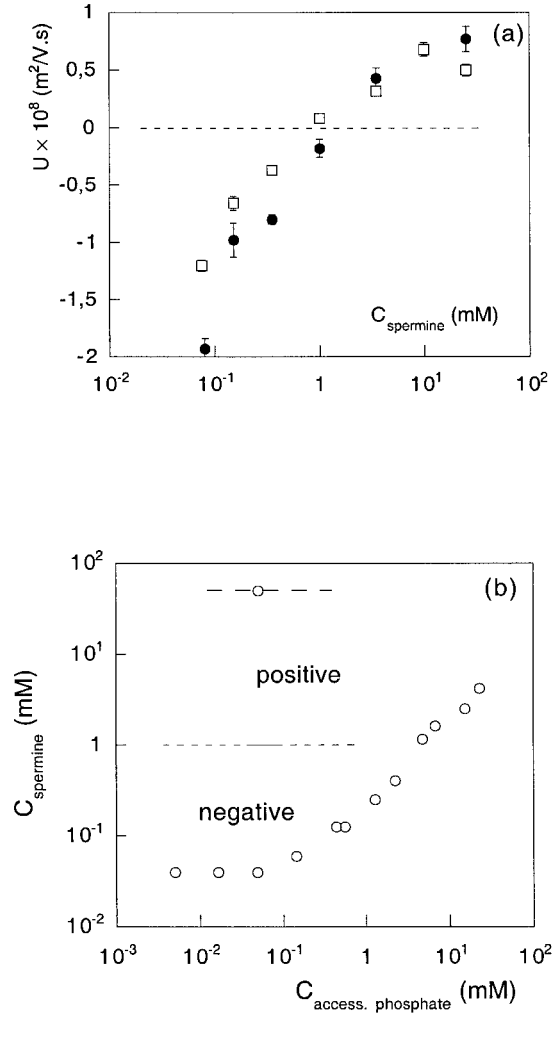

FIGURE 7 (*a*) Variation of the electrophoretic mobility of the aggregates of NCP with the spermine concentration in TE buffer + 5 mM NaCl. The dotted line indicates the zero electrophoretic mobility value. The electrophoretic mobility of the aggregates of NCP, formed at accessible phosphate concentrations 0.0825 mM (●) and 0.041 mM (□), increases continuously with the spermine concentration. Aggregates become positively charged above 1 mM spermine. (*b*) Surface charge of the NCP aggregates determined by electrophoretic measurements and reported in the phase diagram. The electrophoretic mobility equals zero at 1 mM spermine and for C_{ap} (mM) = 0.041 and 0.0825. The continuous line joins these two concentrations. We have extrapolated this line on both sides (*dashed line*). The upper dashed line is an extrapolation of the redissolution conditions.

is reversed. The surface charge of the aggregates over the entire phase diagram is indicated in Figs. 6 *b* and 7 *b*.

DISCUSSION

In an intermediate range of polyelectrolyte concentration, the experimental conditions of precipitation are well-described by the "ion-bridging" model (Eq. 1). Our results support the first three theoretical assumptions and predictions presented in the Introduction.

1. The precipitation conditions are independent of the degree of polymerization. This was observed in a previous work for dsDNA (Raspaud et al., 1998) and is extended in the present study for a variety of molecular species (ssDNA, chromatin fragments). This is also in good agreement with the experiments performed with poly(styrene sulfonate) chains (Na-PSS) by Delsanti et al. (1994);
2. The precipitation conditions are independent of the linear charge density ξ of the polyelectrolyte. This is illustrated by the comparison between ss and dsDNA, which have different structural parameters $\xi = 1.8$ and $\xi = 4.2$, respectively;

3. The superimposition of precipitation curves obtained with linear DNA and nucleosome core particles allows us to confirm the independence of the polyelectrolyte shape in the precipitation process. This supports the idea that the electrostatic attractive interactions are purely local.

Bibliographical data further support the idea that our results can be generalized to linear polyelectrolytes. In our experiments, all polyelectrolytes carry the same phosphate groups, and we used only the tetravalent polyamine spermine as a counterion. Similar results were obtained with sulfate and sulfonate chains precipitated by very different trivalent cations (Sabbagh, 1997), spermidine (a linear polycation), or lanthanum (a spherical ion). It means that in a first approach, we do not need to take into account structural specificities to describe the precipitation process. This supports the theoretical approach we used, in which the spermine (4+) is considered as a charged point, which reverses the phosphate charge (1−) into a charge (3+).

We have also extended this study to NCP, which may be viewed as charged colloids. Since the variation of the precipitation conditions for NCP is similar to that of the linear polyelectrolytes in the whole diagram, we think that it is possible to separate the diagram into the same three regions corresponding to different distributions of condensed mono and multivalent counterions. However, it requires a more precise theoretical description of the ionic condensation, which takes into account both structural and polyelectrolyte specificities of these particles. First, their geometry is not rigorously spherical; the nucleosome is a flattened cylinder with a structural anisotropic factor (diameter/height) equal to 1.84. The charge distribution at the surface is not homogeneous because the DNA is coiled around the cylindrical part (Luger et al., 1997). As the NCP are formed by mostly electrostatic protein/protein and protein/DNA attractive interactions, the ionic environment can modify these interactions and the structure of the particles. Under our experimental conditions, the integrity of the NCP is retained and its global shape is not modified, but the basic tails of the histone proteins could be either folded onto the lateral surface, thus interacting with DNA negatively charged, or extended outside. Polyamines are known to induce this extension of certain tails at concentrations lower than the aggregation concentrations (Dumuis-Kervabon et al., 1986; Encontre and Parello, 1988). An extension of the tails would change the ratio of accessible phosphate charges from 0.55 to a maximum value of 0.71. However, a variation of the accessible phosphate charges would not alter our results within the precision of our measurements.

Similar studies have already been performed in other colloidal systems. For example, in the case of silica dispersion, different values of the critical coagulation concentration (CCC) of iron (III) have been reported as a function of the colloid concentration for different pH values (Stumm and O'Melia, 1968). The authors report a proportionality between the colloidal concentration and the CCC, which suggests that this phenomenon would be a general rule for charged colloids. However, it remains difficult to draw a direct comparison of their data with ours because the surface charge density per colloid is unknown, and because hydrolysis effects of the metal cations provoke subsequent polymerization effects.

These conditions seem thus to be general and well-described by Eq. 1. However, in detail, a discrepancy appears between experiments and theoretical predictions, as enlightened by the representation given in Fig. 5. Experimental data can be averaged by a constant 0.20 ± 0.02, which is not understood on account of the model that has been used. This suggests that precipitation occurs for a constant fraction of spermine condensed onto the polyelectrolyte. Yet, theory predicts that instability conditions may occur in the region b whatever the fraction of condensed spermine (i.e., whatever the ratio C_{sper}/C_{ap}) leading to a theoretical curve (Fig. 5), which decreases continuously when C_{ap} increases. Three hypotheses can be proposed to explain this discrepancy:

1. The precision of the experiments is ~10%, which is perhaps not enough to detect this decrease. More precise experiments (with smaller intervals) should be done on a larger range of polyelectrolyte concentration (polyelectrolytes with a lower charge density to extend the region b toward higher concentrations and polyelectrolytes with a higher charge density to extend it toward the lower concentration side);
2. The theoretical decrease may be overestimated. This results from the simplified Manning theory, which is expressed in its limiting form and becomes less relevant at high polyelectrolyte concentration. The two variables, Manning's theory (in the case of linear chains) or the Poisson-Boltzmann theory may be better used instead;
3. Precipitation could be better-described by the coexistence curve in the high polyelectrolyte concentration range rather than by the spinodal equation, as already mentioned (Raspaud et al., 1998).

In Fig. 5, for high chromatin concentrations, precipitation conditions are still located in region b and deviate by >10% from the theoretical curve, which would rather support hypotheses 2 or 3. Nevertheless, the prefactor used in this case to relate C_{NCP} to C_{ap} comes from an estimation and could induce a translational error in the figure. This prefactor may also depend on the concentration and introduce an artefactual increasing gap between experiments and theory.

The theoretical approach developed in Raspaud et al. (1998) relies on a simplified model whose interest is to give an analytical expression (Eq. 1) describing our results. The simple formulation of the model allowed us to expect a generalization that is verified here. However, other theoretical approaches could also predict this behavior. For example, the approach proposed by Stumm and O'Melia (1968) for colloids relies on a "chemical bridging model." The authors use the ion adsorption/desorption notion, which can be compared to the condensation/decondensation notion; this introduces an all-or-none process instead of an ion

concentration gradient. Based on such an adsorption/desorption reaction equilibrium, the authors found a constant ratio between the ion and colloid concentrations when all the ions are adsorbed. This ratio reflects the fraction of the colloidal charges neutralized and is equivalent to the constant ratio C_{precip}/C_{DNAp} found in region b. When there are both free and adsorbed ions, the adsorption/desorption model also gives an expression equivalent to our relationship $\alpha + \beta \times C_{DNAp}$ in region c. Nevertheless, this approach cannot explain the resolubilization process that is observed in these systems and will be discussed elsewhere.

The last point deals with the assumption 4: the instability is expected to occur before the electroneutrality. Our experimental results suggest that two lines have to be distinguished: the line along which the first neutral germs nucleate and the line which corresponds to the electroneutrality of all chains. The first one (partial electroneutrality) superimposes to the precipitation line, whereas we assume the second one (total electroneutrality) to correspond to the line of maximum of precipitation. With DNA short fragments and nucleosome core particles, these two lines are easily distinguished experimentally (see Figs. 6 *b* and 7 *b*). Other complementary experiments should be settled to clarify this assumption in the case of long chains.

In our mobility experiments, only aggregates contribute to the signal. Furthermore, only the charges located at the surface of the aggregates contribute to their mobility. The peripheral layer of the dsDNA and NCP aggregates therefore remains negatively charged between the two lines defined above, the total electroneutrality occurring at 1 mM (for NCP) and 2 mM (for dsDNA) spermine.

Above this electroneutrality line there is no detectable charge reversal for dsDNA aggregates, even close to the redissolution line. Aggregates remain neutral. On the contrary, the surface of the NCP aggregates becomes positively charged. This is not predicted by the ion condensation models. What could explain this difference of behavior between dsDNA and NCP? The phosphate charges, being roughly neutralized by the spermine molecules (as deduced from the behavior of DNA), we suspect that the positively charged proteic tails extend out of the particle and give this positive total charge to the NCP. This effect of the tails could also qualitatively explain the shift in the spermine concentration required for the electroneutrality (from 2 to 1 mM): the positive charges of the tails would counterbalance the DNA phosphate still negatively charged. Thus, the total charge of NCP would be controlled by the negative charges of the DNA phosphate groups below 1 mM and by the positive charge of the proteic tails above 1 mM. One may expect the same behavior with H1-depleted chromatin: the total electroneutrality should occur at a spermine concentration intermediate between 1 and 2 mM because of the presence of linker DNA between NCP particles. It is likely that NCP remain positively charged after resolubilization in excess of cations, and one would expect the same behavior in the case of chromatin, as already suggested by early experiments of Bungenberg de Jong (1949). An analogous situation, with a charge reversal of the aggregate, was reported in other colloid systems (for instance, see Mabire et al., 1984). In this case, the charge reversal is due to an excess of cationic polymer adsorption onto the colloidal surface. Flocculation also starts before complete neutralization of the colloids and total electroneutrality is observed at the maximum of the flocculation.

In the range of DNA concentration where mobility experiments have been performed (regime c), the line of maximum of precipitation (total electroneutrality line) depends on the monovalent salt concentration (Fig. 8), but not on the DNA concentration (Fig. 6 *b* for dsDNA). The presence of added monovalent salts is responsible for the high spermine concentrations at which total neutrality occurs. This indicates the presence of an excess of spermine in the solution, which is due to the competition with the monovalent added salts. At the surface of the aggregates (peripheral layer), mono and multivalent cations compete to condense onto the chains. Higher spermine concentrations are necessary to displace Na^+ ions. Experimentally, we cannot exclude that, in the central part of the aggregates, a fraction of the Na^+ ions remains trapped, although this has not been considered in the simplified model using the limiting laws of ion condensation predicted by Manning. Complementary experiments should now be undertaken to determine the precise ionic composition and distribution within the core of the aggregates.

As a conclusion, we have shown that in an intermediate concentration regime, the precipitation conditions are similar whatever the DNA state: from flexible chains to rigid rods and quasi-colloidal particles, as predicted by the "ion-bridging" model. Our results suggest that the precipitation occurs when ~80% of the accessible charges are neutralized by spermine molecules. In this regime, one expects

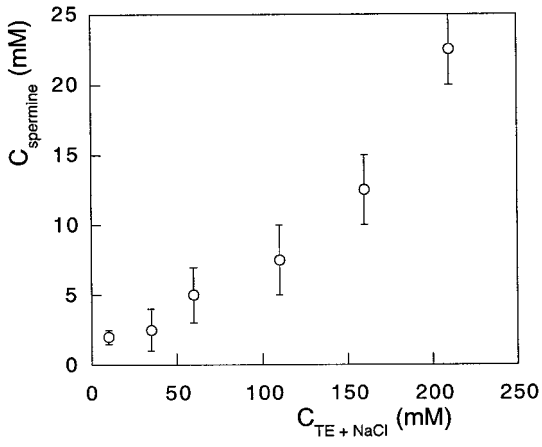

FIGURE 8 Conditions required to induce the maximum precipitation of dsDNA fragments as a function of the added monovalent salt concentration. These conditions, which we assume to correspond to the total electroneutrality line, do not depend on the DNA concentration in the studied range. The values are deduced from the electrophoretic measurements in the case $C_{TE+NaCl} = 10$ mM and from measurements of DNA concentration in the supernatant in the other cases.

chromatin to precipitate, self-aggregate, or fold following the same criterion. Taking into account the concentration of the phosphate charges in the eucaryotic nucleus (assuming a homogeneous distribution of chromatin in the volume), the average spermine concentration required to induce a complete aggregation of chromatin would be larger than the concentration known to exist in the nucleus (in the millimolar range, Bloomfield et al., 1999). This allows polyamines to play a role in regulating the degree of condensation of chromatin by simple fluctuations of their concentration. Because the local ionic fluctuations can determine the surface charge of chromatin, the nucleosomic chain can be envisioned as a succession of domains, either positive, negative, or neutral, in dynamic equilibrium.

This work greatly benefited from stimulating discussions with Monica Olvera de la Cruz. We also thank Bruno Lartiges, who introduced us to the field of colloidal polyelectrolytes; Bruno Pitard, who allowed us to perform the electrophoretic measurements in his group; Dominique Durand for discussions on nucleosome core particle conformations; and Jean-Louis Sikorav for comments on the manuscript.

This work was supported in part by a grant from the Ministère de l'Enseignement Supérieur et de la recherche (ACC-SV5).

REFERENCES

Alexander, S., P. M. Chaikin, P. Grant, G. J. Morales, P. Pincus, and D. Hone. 1984. Charge renormalisation, osmotic pressure, and bulk modulus of colloidal crystals: theory. *J. Chem. Phys.* 80:5776–5781.

Belloni, L. 1982. Interactions electrostatiques dans les solutions aqueuses de polyelectrolytes. Doctoral Thesis. University of Paris VI, France.

Belloni, L. 1985. A hypernetted chain study of highly asymmetrical polyelectrolytes. *Chem. Phys.* 99:43–54.

Bloomfield, V. A., D. M. Crothers, and I. Tinoco, Jr. 1999. Polymer and polyelectrolyte behavior of DNA. *In* Nucleic Acids: Structure, Properties and Function. V. A. Bloomfield, D. M. Crothers, and I. Tinoco, Jr., editors. University Science Books, Mill Valey, CA. In press.

Bloomfield, V. A., C. Ma, and P. G. Arscott. 1994. Role of multivalent cations in condensation of DNA. *ACS Symp. Ser.* 548:185–209.

Bucci, S., C. Fagotti, V. Degiorgio, and R. Piazza. 1991. Small-angle neutron-scattering study of ionic-nonionic mixed micelles. *Langmuir*. 7:824–826.

Bungenberg de Jong, H. G. 1949. Complex colloid systems. *In* Colloid Science, Vol. 2. H. R. Kruyt, editor. Elsevier Science Publishing Co., New York. 280–283.

Chaperon, I., and J.-L. Sikorav. 1998. Renaturation of condense DNA studied through a decoupling scheme. *Biopolymers*. 49:195–200.

Clark, D. J., and T. Kimura. 1990. Electrostatic mechanism of chromatin folding. *J. Mol. Biol.* 211:883–896.

Delsanti, M., J. P. Dalbiez, O. Spalla, L. Belloni, and M. Drifford. 1994. Phase diagram of polyelectrolytes solutions in presence of multivalent salts. *ACS Symp. Ser.* 548:381–392.

Dumuis-Kervabon, A., I. Encontre, G. Etienne, J. Jauregui-Adell, J. Mèry, D. Mesnier, and J. Parello. 1986. A chromatin core particle obtained by selective cleavage of histones by clostripain. *EMBO J.* 5:1735–1742.

Encontre, I., and J. Parello. 1988. Chromatin core particle obtained by selective cleavage of histones H3 and H4 by clostripain. *J. Mol. Biol.* 202:673–676.

Khrapunov, S. N., A. I. Dragan, A. V. Sivolob, and A. M. Zagariya. 1997. Mechanisms of stabilizing nucleosome structure. Study of dissociation of histone octamer from DNA. *Biochim. Biophys. Acta*. 1351:213–222.

Leforestier, A., and F. Livolant. 1997. Liquid crystalline ordering of nucleosome core particles under macromolecular crowding conditions: evidence for a discotic columnar hexagonal phase. *Biophys. J.* 73: 1771–1776.

Luger, K., A. W. Mäder, R. K. Richmond, D. F. Sargent, and T. J. Richmond. 1997. Crystal structure of the nucleosome core particle at 2.8 Å resolution. *Nature*. 389:251–260.

Mabire, F., R. Audebert, and C. Quivoron. 1984. Flocculation properties of some water-soluble cationic copolymers toward silica suspensions: a semiquantitative interpretation of the role of molecular weight and cationicity through a "patchwork" model. *J. Colloid Interface Sci.* 97: 120–136.

Manning, G. S. 1978. The molecular theory of polyelectrolyte solutions with applications to the electrostatic properties of polynucleotides. *Q. Rev. Biophys.* 11:179–246.

Marquet, R., A. Wyart, and C. Houssier. 1987. Influence of DNA length on spermine-induced condensation. Importance of the bending and stiffening of DNA. *Biochim. Biophys. Acta.* 909:165–172.

Olvera de la Cruz, M., L. Belloni, M. Delsanti, J. P. Dalbiez, O. Spalla, and M. Drifford. 1995. Precipitation of highly charged polyelectrolyte solutions in the presence of multivalent salts. *J. Chem. Phys.* 103: 5781–5791.

Pelta, J., F. Livolant, and J.-L. Sikorav. 1996. DNA aggregation induced by polyamines and cobalthexamine. *J. Biol. Chem.* 271:5656–5662.

Ramanathan, G. V. 1988. Counterion condensation in micellar and colloidal solutions. *J. Chem. Phys.* 88:3887–3892.

Raspaud, E., M. Olvera de la Cruz, J.-L. Sikorav, and F. Livolant. 1998. Precipitation of DNA by polyamines: a polyelectrolyte behavior. *Biophys. J.* 74:381–393.

Record, M. T. Jr., C. P. Woodbury, and T. M. Lohman. 1976. Na+ effects on transitions of DNA and polynucleotides of variable linear charge density. *Biopolymers.* 15:893–915.

Sabbagh, I. 1997. Stabilité de polymères anioniques en présence de cations multivalents. Doctoral Thesis. University of Paris VII, France.

Saminathan, M., T. Anthony, A. Shirahata, L. H. Sigal, T. Thomas, and T. J. Thomas. 1999. Ionic and structural specificity effects of natural and synthetic polyamines on the aggregation and resolubilization of single-, double-, and triple-stranded DNA. *Biochemistry*. 38:3821–3830.

Sikorav, J.-L., J. Pelta, and F. Livolant. 1994. A liquid crystalline phase in spermidine-condensed DNA. *Biophys. J.* 67:1387–1392.

Smirnov, I. V., S. I. Dimitrov, and V. L. Makarov. 1988. Polyamine-DNA interactions. Condensation of chromatin and naked DNA. *J. Biomol. Struct. Dyn.* 5:1149–1161.

Strzelecka, T. E., and R. L. Rill. 1987. Solid-state 31P NMR studies of DNA liquid crystalline phases. The isotropic to cholesteric transition. *J. Am. Chem. Soc.* 109:4513–4518.

Stumm, W., and C. R. O'Melia. 1968. Stoichiometry of coagulation. *J. A. W. W. A.* 60:514–539.

Tang, J. X., S. Wong, P. T. Tran, and P. A. Janmey. 1996. Counterion induced bundle formation of rodlike polyelectrolytes. *Ber. Bunsenges. Phys. Chem.* 100:796–806.

van Holde, K. E. 1989. Chromatin. A. Rich, editor. Springer-Verlag Inc., New York.

Watanabe, K., and K. Iso. 1984. Magnesium binding and conformational change of DNA in chromatin. *Biochemistry.* 23:1376–1383.

Wilson, R. W., and V. A. Bloomfield. 1979. Counterion-induced condensation of deoxyribonucleic acid. A light-scattering study. *Biochemistry*. 18:2192–2196.